J. Synchrotron Rad. (1999). **6**, 198–200

In situ EXAFS study of nickel hydroxide electrodes during discharge

N.R.S.Farley, S.J.Gurman, A.R.Hillman*

Department of Physics, University of Leicester, Leicester LE1 7RH, UK
** Department of Chemistry, University of Leicester*

The energy dispersive EXAFS technique has been used to determine the structure of a nickel hydroxide film *in situ* during the discharge process. Each measurement of the nickel K-edge absorption took approximately 150 s so that the process could be followed accurately. We report changes in the energy of the nickel edge, which gives the charge state of nickel ions in the electrode, and changes in the local structure around the nickel atoms during the discharge process. These variations are correlated with the total charge on the electrode.

Keywords: nickel hydroxide, energy dispersive X-ray absorption spectroscopy, electrochemistry.

1. Introduction

Extended X-ray absorption fine structure (EXAFS) in the energy dispersive mode (EDE) is a useful technique for the *in situ* study of redox processes in real time. The redox properties of electrochemically prepared (ECP) nickel hydroxides have been investigated extensively due to their importance as battery and fuel-cell materials (Saville *et al.*,1997 and Olivia *et al.*,1982). Previous time-resolved EXAFS studies of the nickel hydroxide system have explored these applications by using plastic-bonded electrode preparations to investigate structural changes during potential cycling (Guay *et al.*,1991 and O'Grady & Pandya, 1994). Here, we describe a simple thin-layer cell in which the structural modifications that accompany the overcharge and discharge of nickel hydroxide films can be monitored as a function of time. This preliminary work can therefore prove useful for the development of electrochromic devices (Scarminio *et al.*,1992) where *in situ* structural studies of transition metal oxide films are required.

EXAFS is a technique which is commonly used to obtain short-range structural information. This is especially beneficial for electrochemically deposited films that have little order further than the molecular level, and therefore fail to provide conclusive X-ray diffraction patterns. Recent work on many chemically prepared (CP) nickel oxides has shown that a linear relationship exists between the first Ni-O distance and Ni valency (Mansour & Melendres, 1997). A calibration curve can therefore be constructed from a linear fit to the Ni-O distances of these well-crystallised standard compounds of varying Ni valency. *In situ* EXAFS measurements have shown that a considerable contraction of the first Ni-O distance takes place when the nickel (hydr)oxide electrode (NOE) is oxidised (O'Grady & Pandya, 1994). When this bond length is placed on the calibration curve, an oxidation state between +3 and +4 is indicated (Capehart *et al.*,1991 & O'Grady *et al.*, 1996). This is corroborated by observing an analogous, previously established linear shift in the Ni K-edge energy to higher values with increasing Ni valency (Mansour *et al.*, 1994). In our work, both the near edge structure (XANES) and EXAFS are used to construct such calibration curves in order to interpret the behaviour of nickel hydroxide films as they are overcharged and then discharged.

EDE is an ideal technique for studying the discharge process because a set of good quality absorption spectra can be obtained in timescales around 2 mins (each spectrum having a acquisition time as short as 3 ms). This mode requires the use of a triangular Si crystal that is cylindrically bent in order to produce a polychromatic beam of the required energy range. This is achieved because the incoming X-rays are reflected off the curved crystal at varying Bragg angles. The curvature of the crystal then serves a dual purpose by focusing the dispersed beam onto the sample at the focal point, before it diverges toward a position sensitive detector (Dartyge *et al.*,1984).

A cell that meets spectroscopic, electrochemical and practical demands must provide for the following requirements: From a spectroscopic point of view, a design that prevents excessive beam attenuation, absorption and scattering is essential. A three electrode arrangement that will not accentuate these effects but does exhibit a geometry suitable for accurate and dynamic potential control and measurement provides for spectroscopic and electrochemical needs. For practical reasons, the cell should consist of cheap and readily available materials that are strong and inert. The cell itself must allow for precise positioning and its components should be easily assembled, dismantled and cleaned. The reported cell meets all of the above criteria, thus providing a means for measuring changes in the EDE-derived structural parameters under conditions in which the potential, and hence the current and charge of the NOE vary.

2. Experimental

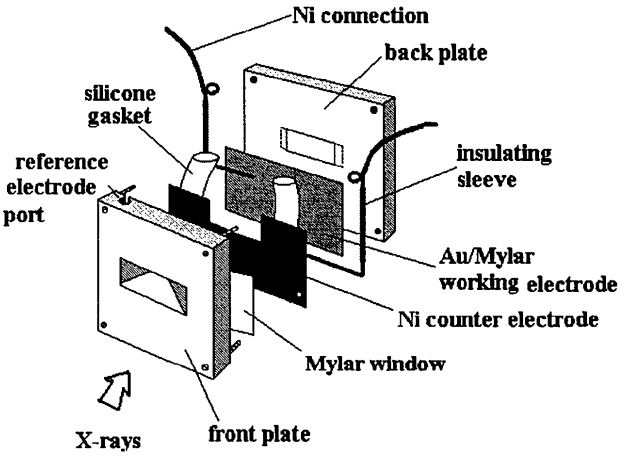

Figure 1
Exploded view of X-ray absorption spectroelectrochemical cell.

Cell: The *in situ* cell (fig.1) consisted of perspex front and back plates (5x5x1 and 5x5x0.5 cm^3 respectively). The front and back window openings were cut with sides slanting inward and outward at 45°, respectively, to allow for fluorescence detection at either side of the cell. The back opening was slightly larger to allow the beam to leave the cell with minimal scatter. Mylar windows were affixed to the plates using epoxy resin. Ni wires (0.5 mm diameter) were used as connections to the Au-coated Mylar working electrode and the Ni foil counter electrode (0.05 mm thick) sandwiched between the two plates. These wires were sleeved to prevent shorting whilst in the thin layer arrangement. The working electrode connection was placed next to the window area to ensure that accurate control and measurement of potential was achieved over the illuminated area. A U-shaped silicone gasket served to separate the working and counter electrodes and formed a flexible seal that prevented leakage. This created a U-shaped cavity that was compressed using stainless steel screws,

restricting the cell thickness to 2 mm; resulting in an electrolyte volume of 1 cm^3 and an electrochemically active working area of 8.5 cm^2. The Hg/HgO reference electrode slotted into a port in the front plate that ended at the top of the window. The full length of this port opened into the cell cavity, thus full contact with the electrolyte was facilitated.

Film preparation: Electrochemical control was accomplished using an Oxford Electrodes potentiostat with a Keithley 175A autoranging multimeter and an Advance Bryans series 60000 X-Y recorder. $Ni(OH)_2$ films were deposited cathodically from 0.1M $Ni(NO_3)_2$ solution at -1.0V *vs.* Hg/HgO for 1hr to give films about 5μm thick and Ni edge steps of ~1.5. The substrates consisted of Mylar with an approximately 1000Å thick evaporated layer of Au (12 cm^2) fixed to the back plate of the cell. Once deposited, the films were gently rinsed with triply distilled water before the cell was assembled, filled with degassed 1.0M KOH and sealed with Parafilm (a maximum duration of 10 mins).

Electrochemistry: Overcharge of a fresh $Ni(OH)_2$ film was carried out by slowly increasing the anodic potential from open circuit to 0.50 V and then holding it there for 2 hrs. Overcharged films were then discharged at 0 V during which the current was measured and spectra were taken.

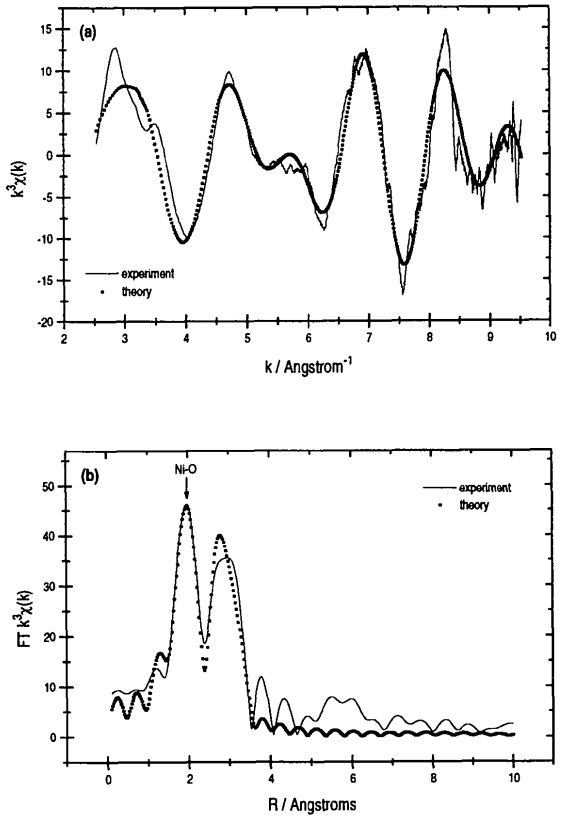

Figure 2
(a) k^3 EXAFS fit and (b) its fitted Fourier transform, for the overcharged electrode.

EDE: Absorption spectra were acquired on beamline 9.3 of the CLRC Daresbury Laboratory (Cheshire, UK) operating at an electron energy of 2 GeV and a ring current of ~125 mA. The energy dispersive instrumentation utilised a curved Si(220) crystal and a Reticon RL1024S linear photodiode array detector. The beam was applied through the front of the cell. Spectra were taken at room temperature (20±1°C) between 8200 and 8800eV, after energy calibration at the Ni K-edge using a 5 μm thick Ni foil. Each raw spectrum consisted of the of the sum of 2000 25 ms scans. Spectra were acquired throughout the full discharge process. Pre and post-edge background was subtracted using polynomial fits (EXBACK). The background subtracted spectra were fitted using the Daresbury program EXCURV97. This uses the fast curved wave theory (Gurman *et al.*,1984) with scattering data within the program from a Hedin-Lundqvist potential. k^3 weighting was applied. Structural parameters fitted were the interatomic distance R, Debye-Waller factor σ^2 and coordination number N. Both split and unsplit Ni-O shells were tried. Typical fits to the EXAFS in k and R space are shown in fig.2 (a and b, respectively).

All analyses were coupled with those of an ECP film that was soaked in electrolyte for several hours. This is because the film may have aged during the course of discharge. Any structural changes induced by the process were therefore accounted for.

3. Results and discussion

Characterisation: When cycled between -0.15 and 0.56 V *vs.* Hg/HgO at 20 mVs^{-1}, both freshly prepared and overcharged films exhibited cyclic voltammograms characteristic of the $Ni(OH)_2$/NiOOH couple (Streinz *et al.*,1995). Overcharge of a fresh film induced the expected electrochromic response for the formation of NiOOH *i.e.* black colouration. This was not completely reversed at discharge, indicating that some Ni atoms remained in a charged state, even when the discharge current was zero.

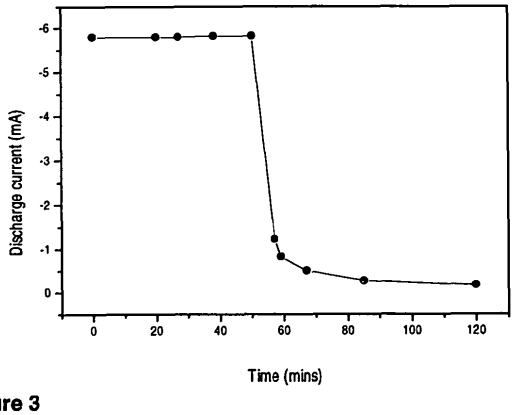

Figure 3
Current-time profile of discharging NOE and the points (dots) at which spectra were taken.

Fig.3. shows the measured discharge current as a function of time after overcharge of a fresh film; the dots represent spectral acquisition. The current plateau before 25 mins is due to current limitation by the potentiostat. The total charge passed was about 20 C for both the charge and discharge process. This charge corresponds to one electron transfer per nickel atom. The XANES and EXAFS of various chemically prepared standard Ni oxycompounds were also analysed.

Fig.4. is a calibration curve defined by the shift in edge position (measured as half the height of the raw spectrum edge jump) relative to that of Ni foil for CP nickel oxycompounds at several oxidation states. From this plot, an edge shift of about 1.6 eV per unit change in Ni valency is calculated. When fixed to the calibration curve, the edge shift of the freshly prepared electrode relates to a Ni valency between +2 and +3; though its value is

slightly higher than that of the standards in the same range (CP-$Ni(OH)_2$ and NiO). Overcharging increases the Ni oxidation state to between +3 and +4. The overall Ni valency of the discharged NOE is essentially the same as the fresh electrode, suggesting that the NOE reverts to its original charge state once overcharge ceases.

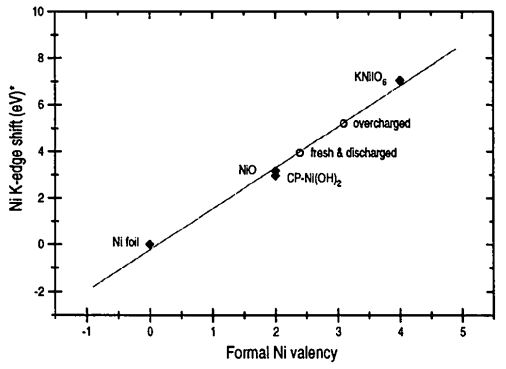

Figure 4
Shift in Ni K-edge with increasing Ni charge state. Diamonds represent Ni foil and CP- standard oxycompounds (spectra taken in standard transmission mode). Circles represent NOEs.
* Shift is measured as the difference between the sample and its corresponding Ni foil edge position.

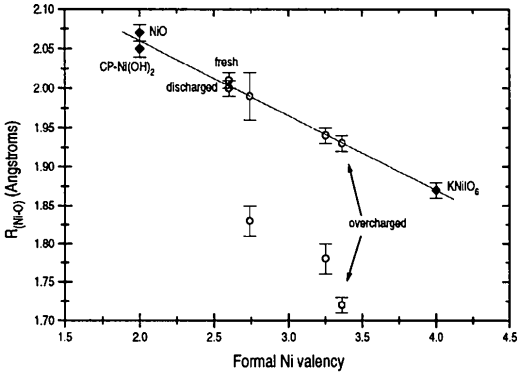

Figure 5
First Ni-O shell distance as a function of Ni valency for CP- (diamonds) and ECP- (circles) oxycompounds.

Fig.5. is a calibration curve showing how the distances in the first Ni-O shell vary with Ni valency. A linear fit to the bondlengths from the standards defined the calibration curve, onto which the NOE bondlengths were fixed. It can be seen that the fresh NOE exhibits a single (6-coordinate) Ni-O bond length. When fixed to the calibration curve, it corresponds to a Ni oxidation state between +2 and +3. The first Ni-O shell becomes distorted on overcharge (a 2-long, 4-short distortion of the octahedral NiO_6 environment), indicating an overall Ni valency between +3 and +4. The bond lengths derived from our *in situ* measurements demonstrate that this distortion reverses during the discharge process; thus returning the Ni-O shell to its original configuration, and implying a reversion to the original Ni valency. Fig.5 therefore confirms the trends indicated by fig.4.
The results derived from simultaneous *in situ* acquisitions of spectra and current readings are represented in fig.6. Four stages in the NOE's structural development are demonstrated; the fresh, overcharged, discharging, and discharged electrode. Distortion of the first Ni-O shell is dependent upon charge and is at a maximum on overcharge. The extent of distortion decreases when electrode charge falls, shown by the convergence of the 2 Ni-O distances during discharge (expressed by the lines on fig.5). A comparison of figures 5 and 6 therefore confirms the relationship between mean Ni valency and charge on the electrode.

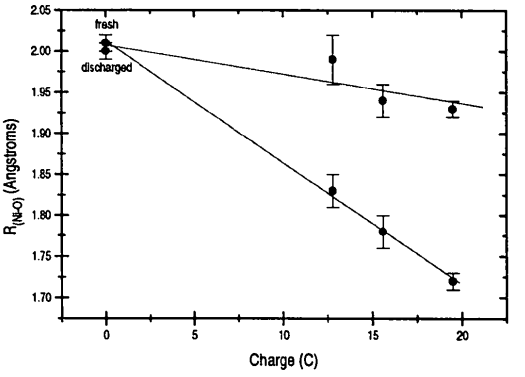

Figure 6
First Ni-O shell distances as a function of charge on the electrode. The lines are linear fits to the two sets of bond lengths.

None of the stated parameters changed significantly for films left to age in electrolyte. Therefore, ageing over these timescales bore no notable influence upon the reported results. This work has used energy dispersive EXAFS to shed light upon the previously unknown transition occurring between overcharge and full discharge. A mechanism for the full structural evolution of the NOE can eventually be completed, thereby providing an understanding which is of vital importance to electrochromic device and battery technology.

The authors acknowledge the EPSRC for financial support, and Dr. A.J.Dent at Daresbury Laboratory for assistance with the EDE setup.

References

Capehart T.W., Corrigan D.A., Connell R.S., Pandya K.I. & Hoffman R.W., (1991) *Appl. Phys. Lett.*, **58** (8), 865-867.
Dartyge E., Fontaine A., Jucha A. & Sayers D., (1984) *EXAFS and Near Edge Structure III*, K.O.Hodgson, B.Hedman & J.E.Penner-Hahn (eds.), pp 472-475, Springer-Verlag, Berlin.
Guay D., Tourillon G., Dartyge E., Fontaine A., McBreen J., Pandya K.I. & O'Grady W.E., (1991) *J.Electroanal. Chem.*, **305**, 83-95.
Gurman S.J., Binsted N. & Ross I., (1984) *J.Phys C*, **17**, 143-152.
Mansour A.N. & Melendres C.A., (1997) *J. Phys. IV France, J.de Physique IV*, **7** (C2), 1171-1172.
Mansour A.N., Melendres C.A., Pankuch M. & Brizzolara R.A., (1994) *J.Electrochem. Soc.*, **141** (6), L69-L71.
O'Grady W.E., Pandya K.I., Swider K.E. & Corrigan D.A., (1996) *J.Electrochem. Soc.*, **143** (5), 1613-1616.
O'Grady W.E. & Pandya K.I., (1994) *Synchrotron Techniques in Interfacial Electrochemistry*, C.A.Melendres & A.Tadjeddine (eds.), pp 247-261, Kulwer, Netherlands.
Olivia P., Leonardi J., Laurent J.F., Delmas C., Braconnier J., Figlarz M., Fievet M. & de Guibert A., (1982) *J.Power Sources*, **8**, 229-255.
Saville P.M., Gonsalves M., Hillman A.R., Cubitt R., (1997), *J. Phys. Chem. B*, **101** (1), 1-4.
Scarminio J., Estrada W., Andersson A., Gorenstein A. & Decker F., (1992), *J. Electrochem. Soc.*, **139** (5), 1236-1239.
Streinz C.C., Hartman A.P., Matupally S. & Weidner J.W., (1995) *J.Electrochem. Soc.*, **142** (4), 1084-1089.

(Received 10 August 1998; accepted 22 January 1999)